VNU Journal of Science: Earth and Environmental Sciences
Journal homepage: https://js.vnu.edu.vn/EES

Original Article

Facile and Effective Synthesis of Non-nobel Metal Oxide Composite Heterojunction Catalyst for CO_2 Reduction Reaction

Le Duc Anh[1,2,*], Jenaidullah Batur[1], Sebghatullah Mudaber[1]

[1]*Beijing University of Technology, 100 Pingle Road, Chaoyang District, Beijing 100124, P. R. China*
[2]*Vietnam National Institute of Occupational Safety and Health, 99 Tran Quoc Toan, Hoan Kiem, Hanoi, Vietnam*

Received 27th August 2024
Revised 14th November 2024; Accepted 29th April 2025

Abstract: Increasing CO_2 emmision leads to global warming. Effective and impotent strategies such as photocatalytic CO_2 reduction and utilization was proposed to solve this issue by using sustainable solar energy. We provided a novel, facile, and eco-friendly synthesis strategy to effectively synthesize TiO_2-organic composite materials to selectively reduce CO_2 to CO. This strategy not only improves TiO_2 photocatalytic activity but also shows potential to apply with alternate metal oxide composite catalyst.

Keywords: Photocatalyst, Heterogeneous Catalyst, Metal Oxide, TiO_2, Composite Materials.

1. Introduction

Green chemistry and green environment importance are widely increasing in our century. CO_2 emission, water purification, and heavy metal adsorption [1] are also important for industrial and environmental purification. As industrial growth rapidly increased fossil fuel use, parallelly CO_2 emissions increased in the atmosphere. Recent research indicates that over 60% of global warming can be attributed to both natural processes and industrial CO_2 production. The atmospheric concentration of CO_2 was already 48% above pre-industrial levels by 1850. Before the industrial age, the average atmospheric CO_2 concentration ranged from 172 ppm to 300 ppm. However, according to the latest Earth CO_2 report, the concentration has

* Corresponding author.
E-mail address: ducanh.nilp@gmail.com

https://doi.org/10.25073/2588-1094/vnuees.5236

now reached 416.87 ppm as of May 20, 2020 [2], [3]. The alarming rise in CO_2 emissions poses a significant threat to the delicate balance of our natural ecosystems [4, 5]. Urgent action is needed to reduce atmospheric CO_2 levels and mitigate global warming and environmental damage [4] one of effective approaches is CO_2 utilization techniques, with carbon dioxide photoreduction being particularly attractive due to its sustainability, non-toxicity, and abundant availability. Implementing CO_2 photo reduction is straightforward and beneficial.

Currently, there is a list of catalysts that can reduce CO_2 to valuable chemicals and fuels, among them metal oxides such as TiO_2 known as promising photocatalysts to produce hydrogen and CO, unless they are at an earlier age and still need to promote activity to able for produce fabricated values. Titanium (IV) oxide (TiO_2), has been used as catalysts for environmental applications due it its low cost, photocatalytic efficiency, and nontoxicity properties [6]. TiO_2 is used for several environmental experiments, insisted of Nobel metals catalysis with improving charge separation of photogenerated electrons and holes [7] such as environmental cleanup, water splitting, oxidization, reduced water molecules, organic synthesis, west water treatment [8] and, CO_2 photoreduction reaction. The TiO_2 bandgap is larger than 3.0 EV also can able to use for device applications [9], wettability control for self-cleaning [10], and electrochromic windows [11]. Due to its limited photocatalytic activity research, adding impurities can improve the photocatalytic production of TiO_2. His group declared that the Schottky barrier formed at the metal- TiO_2 interface of Ag, Pt, and Au-doped TiO_2, and charge carrier recombination decreased [12, 13]. Cheng et all 2007 reported non-metal-doped TiO_2 (C, N, S, B, P, F, and I) to compare with metal-doped TiO2 [14], they may improve the extension of photocatalytic activity of TiO_2 under visible light due to their impurity state is near the valance bandgap, but they did not act as charge carriers or their role as recombination centre minimized. To improve the nunneries nonmetals- TiO_2 photo catalyst light absorption into visible light has been reported. Among them, N-TiO2 and C-TiO2 nanomaterials have improved photocatalysis activity [15, 16].

Ansari et all reported that the ball milling method can shift the light absorption ability from UV to visible light and red phosphorus can effectively improve the photocatalysis of TiO_2 [17]. TiO_2 nano-wires (Ti-NWs) and nan-flaks (Ti-NFs) Hydrothermal heat treatment increases the optical response and separation of photogenerated charge carriers [20]. We have reported the first, fast, cheap, and effective synthesis method in our previous work [21] and we applied that method to our current work TiO_2/SAC nanocomposite material without using any harmful organic solvent with a low temperature of 80 ^oC. We directly used titanium (IV) dioxide nanocrystals and Saccharin with LiBr salt without any further chemical process and purification. The CO_2 reduction process at the gas–solid interface on TiO_2-Sac-Li composite semiconductors is investigated by functional calculations and several characterization methods. Compared with nanosized TiO_2, the new TiO_2-Sac-Li indeed displays a high CO generation rate of 70.83 μmol/g/h, which is 7 times higher than TiO_2 which shows enhancement in CO_2 reduction and an apparent improvement in charge carrier dynamic. The results indicate that CO_2 can be easily activated by the TiO_2-Sac-Li atoms on the surface. This work innovatively investigates CO_2 reduction in novel composite materials and helps to broaden the applications of composite materials semiconductors. Characterization, photoreduction activity, and mechanism of action of the new TiO_2/SAC/LiBr composite catalyst particles are discussed.

2. Material

Titanium dioxide (TiO_2, 99%) was purchased from Beijing Shiji as nanocrystal powders. Saccharine (SAC) from Energy chemical, Triethylamine (TEA 500 ml, 99%) from Sinopharm Chemical Reagent Co., Ltd,

Water (18.2 μΩ/cm), lithium chloride (LiCl 96%), lithium bromide (LiBr) from Chemical Reagent, all chemical reagents above purchased commercially and used without further purification.

2.1. Synthesis of Metal Oxide/SAC Composite Catalysts

The composite materials were synthesized with a similar method to our previous report. TiO_2 was manually ground with commercial saccharin (300 mg each, mass ratio of 1:1) in mortar and pestle for 10 minutes under air and ambient conditions. The powder named sample N1. The acquired powder is then mixed with deionized water and LiBr salt (e.g., 0.3 mg sample powder in 10 mL water). The mixture was heated in a Teflon-lined stainless steel acid digestion bomb (Zhong Kai Ya Instrument) at 80 °C.

2.2. Characterisation

The prepared sample phase pattern was collected by powder X-ray diffraction XRD-6000 (Rigaku Co) Smart Lab x-ray diffractometer using Cu Ka (λ = 1.5418Å) irradiation (40 kV, 30 mA) in the 2θ range from 20° to 80° with 0.02° scan step. To analyse the morphology and structure of the samples, scanning electron microscopes (SEM; Hitachi SU3500) operated at the accelerating voltage of 20.0 kV, PerkinElmer Fourier-transform infrared spectroscopy (FTIR) was measured using a Shimadzu IRAffinity-1S spectrophotometer. X-ray photoelectron spectroscopy (XPS) was performed on an ESCALAB 250Xi XPS spectrometer (Thermo Fisher Scientific) using Al Kα radiation. The obtained spectra were calibrated based on the C 1s peak at 284.8 eV.

2.3. Catalytic Reaction

The catalytic reaction of the CO_2 reduction test was performed in a closed stainless reactor 120 mL in capacity with a connected top quartz glass for light irradiation. 1.4 mg of composite was weighed in a 60 mL quartz container, added 100 μL of deionized water and sacrificial agent (TEA) 1:1, the mixture was sonicated in a water bath for 5 minutes to attach water with the catalysis. Then, the reactor was filled with air, and the mixture container was evacuated by a pump before executing a carbon dioxide reduction reaction. The system washed with refilling into the reactor (0.1 MPa of pure CO_2, Beijing Beiwen Gas Comp. 99.999%) repeated 10 times. The performance of the provided catalyst was tested under full spectrum irradiation (300 W xenon with photocatalytic wav-length λ > 320 nm and optical density of 2550.4 mW cm^{-2}). To keep the reaction at room temperature and control the temperature inside the reactor, connect cooling water to the reactor and set it at 24 °C. After the reaction, the formed products were collected every 2 hours. Produced CO was analysed by GC (Shimadzu GC2014C) with a TCD detector using argon gas as carrier gas.

3. Results and Discussion

Synthesis and characterisation of TiO_2/SacLi composite materials. The primary contact between materials obtains with grinding in mortal and pestle in 10 minutes. During the grinding of composite materials may instruct with the component. Saccharine is an organic sugar and it seems pesty during the grinding with TiO_2 nanoparticle powder, after 5 minutes of grinding did not observe a pesty feeling, which is probably because TiO_2 nanoparticles covered saccharine molecules and separated on the saccharin chunks.

The morphology of the TiO_2-Sac-LiBr materials provided with SEM, and Figure 1A denoted the ground TiO_2-SAC-LiBr materials. Figure 1A shows that after the hand grinded of the materials the saccharin looks like a large chalk that almost has a clean surface and TiO_2 separated on the saccharin molecules have low interaction with TiO_2 nanocrystals.

The schematic look of the saccharin is shown in Figure 1. The saccharin molecules have 3 oxygen functional groups after the hydrothermal treatment probably Lithium coordinated with the

oxygen of the saccharin molecule similarly to Na-SAC. After milling these composite semiconductors, TiO_2 nanocrystals covered the saccharin molecules and changed the molecule's environment of the TiO_2 nanocrystals. The morphology studies of the materials have been studied in the SEM section. After hydrothermal treatment, TiO_2 nanocrystals interact deeply with saccharine molecules and are covered with the TiO_2 nanocrystals. Moreover, the saccharine molecules have reduced their size after hydrothermal treatment therefore the smaller size of the molecules made stronger instruction between each other. Instruction of smaller molecules also simplifies the electron transfer between molecules and this operation will provide better reduction ability for the semiconductors.

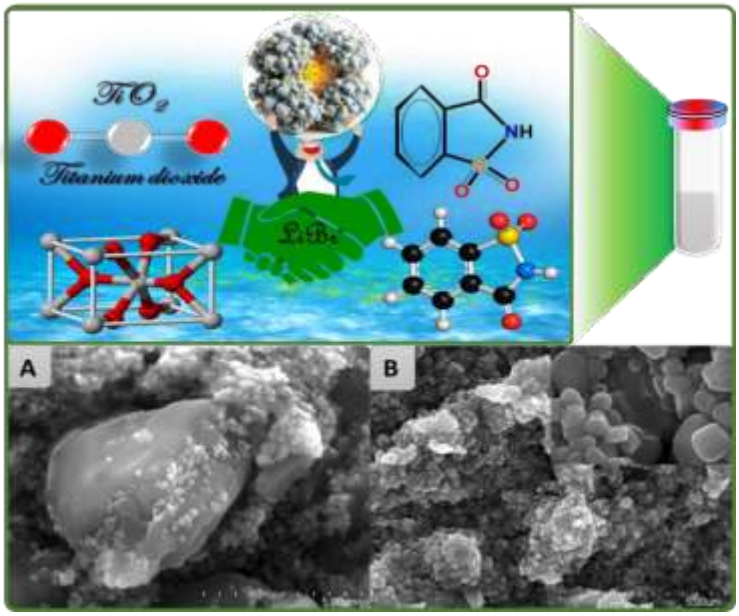

Figure 1. SEM images of (A) TiO_2-Sac-LiBr hand milled, (B) Hydrothermal synthesized TiO_2- Sac-LiBr.

3.1. XPS and FT-IR spectra

X-ray photoelectron spectroscopy (XPS) was utilized to measure compositions and surface functional groups of the composite materials to ensure the surface analysis. The xps peaks has been listed in below.

The measured xps data is as follows: TiO_2 (N0): (C-C and O-C=C Peaks at 284.80, 286.52eV. Ti $2p_{3/2}$ and Ti $2p_{1/2}$ peaks at 459.40, and 465.10 eV. Ti-O and V_o peaks at 530.64 and 532.06 eV). N1: (C-C, C-N, and O-C=C Peaks at 284.80, 285.49, and 288.81 eV. Ti $2p_{3/2}$ and Ti $2p_{1/2}$ peaks at 458.73, and 464.46 eV. Ti-O, Ti-OH, and Vo peak at 529.87, 530.32, and 531.97 eV. Nxps: 398.65, 400.09, 401.58, and S peaks are 168.57 and 169.67 respectively).

N3: (C-C, C-N, and O-C=C Peaks at 284.80, 285.28, and 288.79 eV. Ti $2p_{3/2}$ and Ti $2p_{1/2}$ peaks at 458.69, and 464.42 eV. Ti-O, Ti-OH, and Vo peak at 529.85, 530.46, and 531.91 eV. Nxps: 398.74, 399.97, 401.37, and S peaks are 168.39 and 169.65 respectively). N2: (C-C, C-N, and O-C=C Peaks at 284.80, 285.28, and 288.79 eV. Ti $2p_{3/2}$ and Ti $2p_{1/2}$ peaks at 458.86, and 464.61 eV. Ti-O, Ti-OH, and Vo peak at 531.12, 530.46, and 532.79 eV. Nxps: 398.67, 399.95, 402.31, and S peaks are 168.17 and 169.14 respectively). As shown in Figure 3A, the full XPS shows four peaks of C 1s calibrated according to the reference 284.80 eV. The high-resolution XPS C1s spectra reveal that C exists mostly in the form of C-C and O-C=C in TiO_2 and C-N start to form after the addition of saccharine on TiO_2.

The XPS N 1s spectra could be decomposed into the 3 peaks. As shown in Figure 2d, the deconvolution of the S 2p spectra indicates the presence of the –C–SOx– group, which was located at 168.4 eV and 169.6 eV.

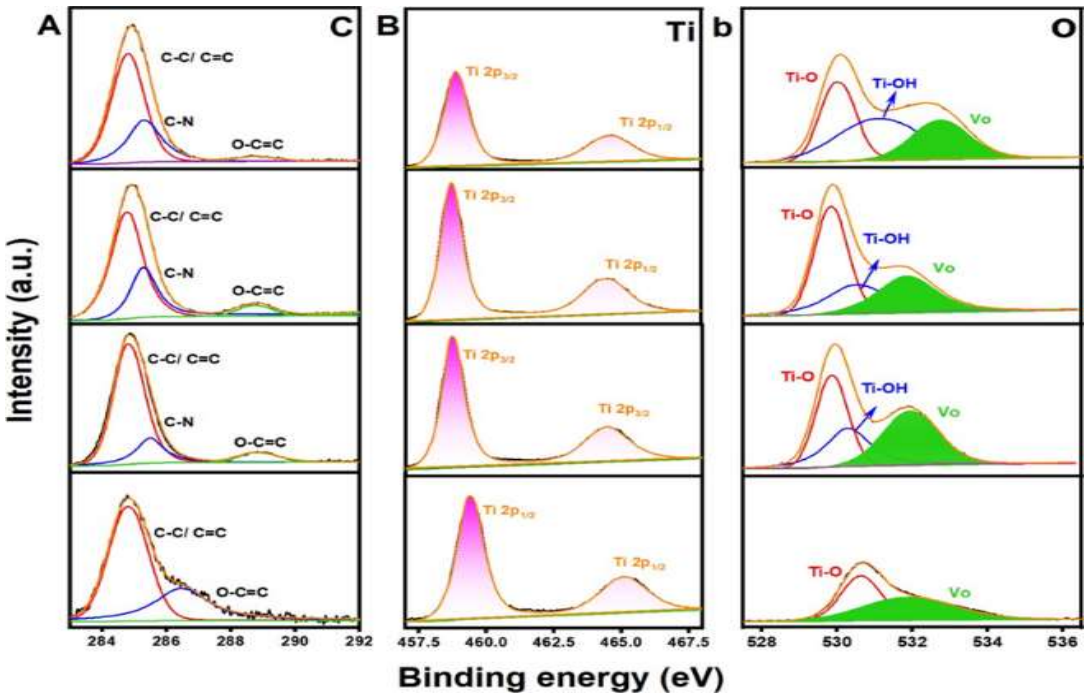

Figure. 2. XPS spectrum of the Carbon (A), Ti (B), and Oxygen (b).

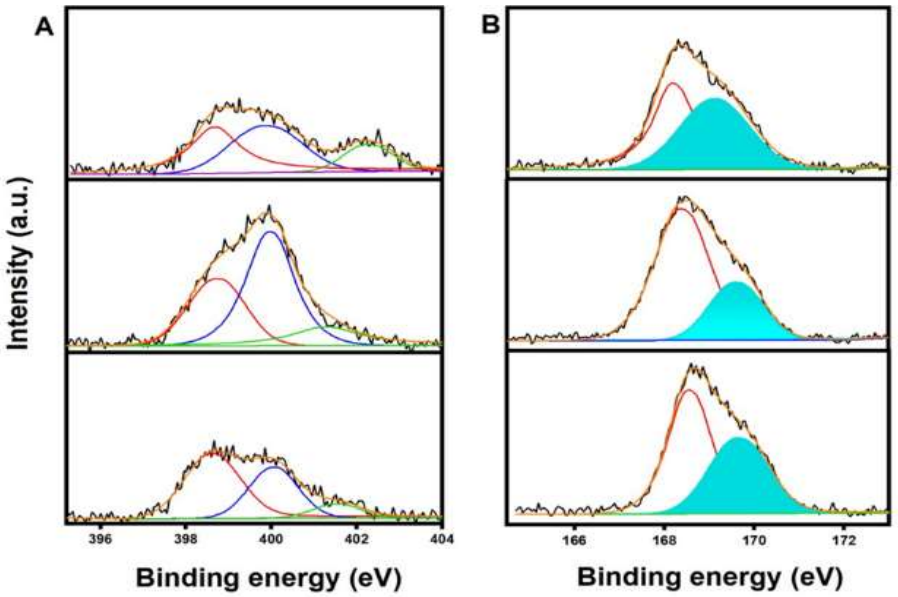

Figure 3. XPS spectrum of Nitrogen (A), and Sulfur (B).

As shown in Figure 4 (4A and 4B), In the FT-IR spectrum of N1 and N2, the peaks at 1269–1126 cm-1 are attributed to the stretching of SO_2 bonds of the saccharin. The peaks at 1684 cm-1 are corresponding to the vibration of carboxylate groups of saccharin molecules. The strong absorption at 1000 cm^{-1} results from the amide bonds of saccharin molecules. the corresponding vibration of these bonds denoted the presence of the saccharin molecules in the composite materials with TiO_2.

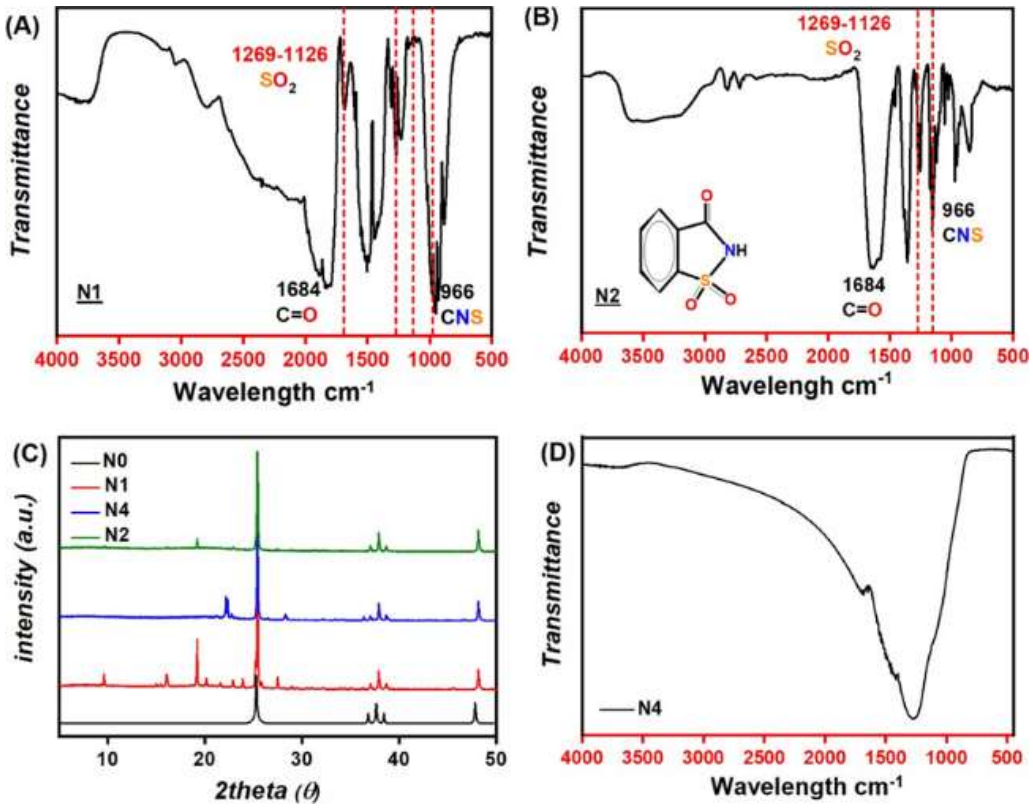

Figure 4. In powder XRD after adding TiO_2 and grinding it some of the XRD peak intensity has decreased showing that saccharine molecules covered TiO_2 nanocrystals. (A) FT-IR spectrum of N1, (4B) N2, (4C) P-XRD pattern of the samples, and (4D) FT-RP spectrum of the N1 after calcination at 500 C.

After heating at 80 ^oC in an autoclave it still shows the characteristic bands of the saccharin in the FT-IR spectrum, some changes have been observed after applying hydrothermal treatment, which may be because of the strong instruction with metal oxide during the heating period. Moreover, after the hydrothermal, the crystal form of the saccharin is impaired and milted and dissolved in the presence of water due to attaching the Li^{+1} it becomes an ionic compound that may dissolve in water and heat. After calcination as shown in Figure 4.D the saccharin molecules were removed from the composite material at 500 C in the presence of oxygen. We did not observe any corresponding vibration band in the FT-IR after the calcination of the catalyst the reason is the oxidation of the saccharin during the calcination with air (O_2) figure. 4D which declared that saccharin molecules are no longer present in the system. due to the saccharin is an organic compound after calcination at 500 C, may decompose at high temperatures. The results after CO_2 reduction reaction experiments have dropped with less production of CO. This result also shows that after removing the saccharin

molecules the P-XRD pattern also conforms to the decomposition of the saccharin after calcination.

This reduction in impedance implies diminished electron-hole recombination, a crucial factor for efficient photoelectron transfer. Our observations collectively confirm the facilitated interphase photoelectron transfer in the semiconductor system. Furthermore, the efficiency of electron conduction followed the order of samples N2>N1. This trend was consistent with their CO_2 reduction reaction (CO_2RR) performance, where the photocatalytic activities of TiO_2-SAC-LiBr significantly outperformed the sample lacking Sac and Li metal (Figure 4B). Importantly, this correlation between catalytic activity and photoelectron transfer efficiency underscores the critical role of the latter as an indicator of interphase contact. Additionally, scanning electron microscopy (SEM) analysis of sample N2 revealed interdigitated TiO_2 on SAC surfaces, signifying decreased interfacial interaction compared to sample N1. These findings provide valuable insights for designing efficient semiconductor systems for energy-related applications.

Our newly synthesized TiO_2-SAC-LiBr heterojunction photocatalyst demonstrates a significant enhancement in CO_2 reduction activity compared to previously reported Ti-based composites, non- metal doped materials, and metal-organic frameworks (MOFs) as evidenced by data in Table 1.

This superior performance is attributed to the presence of the heterojunction, which facilitates efficient charge separation and transfer, extending the lifetime of photogenerated charges that drive the reaction. Additionally, LiBr is postulated to promote CO_2 adsorption and activation on the catalyst surface, further enhancing the overall CO_2RR process. To ensure the catalytic activity of the catalyst applied cycling process. The shows that the catalyst performance after 3rd cycle still unchanged. Notably, the catalyst weight has been reduced after every cycle due the washing the samples that probably effect the activity of CO_2 reduction to CO. Moreover, the application confirmed the catalytic activity of the synthesized composite material. After photocatalyst performance we noticed the high selectivity of the composite catalyst after observing just CO without any other production. The N2 shows higher activity than the Ti and different catalysts reported as shown in the Table 1. The successful application of the metal oxide organic sugar with a green synthesis method verifies a greet step to further usage of the saccharin in term of the industrial application.

Table 1. Photocatalytic CO_2RR Performance of Selected Composite Catalysts Reported in 2020–2022

Composition	Reaction system	Light source	CO (μmol/g/h)	Ref
TiO_2-RP	Water/TEA	300 W Xe Lamp	54.60	[21]
TiO_2/C@ZnCo-Zif-L	Water	300 W Xe Lamp	28.60	[22]
Porous 2D ZnO@g-CN	Water vapor	300 W Xe Lamp $\lambda > 420$ nm	30.50	[23]
P-doped g-C_3N_4	Water	300 W Xe Lamp $\lambda \geq 420$ nm	31.22	[24]
TiO_2-SAC-LiBr	Water/TEA	300 W Xe Lamp	70.83	This work

The promotion of the photocatalytic activity of N_2 over similar composite catalyst indicate the high efficiency of the novel synthesized Ti-SAC composite. The remarkable CO production activity positions the TiO_2-SAC-LiBr composite as a promising candidate for CO_2 reduction applications. Future research can focus on elucidating the underlying mechanisms and optimizing the material's properties to achieve even greater CO production and selectivity, paving the way for scalable and sustainable CO_2RR technologies for a carbon-neutral future.

4. Conclusion

The study aimed to evaluate different methods for preparing composite materials based on TiO_2 and to determine their toxicity profiles and complex methods. Our findings indicate that the presence of organic saccharin and Li metal is a crucial factor in determining the final composite materials. In particular, we found that the inclusion of organic saccharin played a critical role in enhancing the CO_2 reduction rate (CO_2RR) of the composite materials. This observation can be attributed to the fact that organic saccharin contains nitrogen and sulfur, which act as catalytic centres and help facilitate the reduction of CO_2 to CO. Likewise, the incorporation of Li metal also played a crucial role in enhancing the CO_2RR of the composite materials. This can be attributed to the fact that Li metal can act as an electron donor and facilitate the reduction of CO_2 to CO. Moreover, Li metal has a high surface area and can provide a large number of active sites for CO_2 reduction.

Furthermore, we demonstrated that the most effective method to increase the CO_2RR and convert it to CO involves using a grinding and hydrothermal method with water solvent. This method is important to consider as it does not require the use of any organic solvents, which are often toxic and harmful to the environment. Instead, water is used as a solvent, making the method more sustainable and environmentally friendly. These findings highlight the significance of this novel method for preparing TiO_2-based composite materials and its potential benefits for the field of CO_2RR. The method has the potential to be applied in various industrial applications, including the production of fuels and chemicals from CO_2, which can contribute to mitigating climate change and reducing our dependence on fossil fuels. Overall, the study's findings demonstrate the importance of considering the toxicity profiles and complex methods in the preparation of composite materials and the potential benefits of using sustainable and environmentally friendly methods in CO_2 reduction reactions.

References

[1] J. Batur, S. Mudaber, Differences in Heavy Metals Adsorption on Natural, Modified, and Synthetic Zeolites - A Review, Journal of the Turkish Chemical Society Section A: Chemistry, Vol.10, No. 3, 2023, pp. 845-857, https://doi.org/10.18596/jotcsa.2023.

[2] W. Gao, S. Liang, R. Wang, Q. Jiang,Y. Zhang, Industrial Carbon Dioxide Capture and Utilization: State of the Art and Future Challenges, Chemical Society Reviews, Vol.49, 2020, pp. 8584-8686, https://doi.org/10.1039/D0CS00025F.

[3] D. G. Yu, L. N. He, Introduction to CO_2 utilisation. Green Chemistry, Vol. 23, 2021, pp. 3499-3501, https://doi.org/10.1039/D1GC90036F.

[4] H. Sun, A. Wang, J. Zhai, J. Huang, Y. Wang, Impacts of global warming of 1.5 ℃ and 2.0 ℃ on Precipitation Patterns in China by Regional Climate Model (COSMO-CLM), Atmospheric Research Vol. 203, 2018, pp. 83-94, https://doi.org/10.1016/j.atmosres.2017.10.024.

[5] Y. Li, H. Tao, B. Su, Z.W. Kundzewicz, T. Jiang. Impacts of 1.5 °C and 2 °C Global Warming on Winter Snow Depth in Central Asia, Science of the Total Environment, Vol. 651, 2019, pp. 2866-2873, https://doi.org/10.1016/j.atmosres.2017.10.024.

[6] M. Iwase, K. Yamada, T. Kurisaki, O.O. Prieto-Mahaney, B. Ohtani, H. Wakita, Visible-Light Photocatalysis with Phosphorus-Doped Titanium (IV) Oxide Particles Prepared Using a Phosphide Compound, Applied Catalysis B: Environmental Vol, 132, 2013, pp.39-44, https://doi.org/10.1016/j.apcatb.2012.11.014.

[7] E. Doustkhah, M. H. N. Assadi, K. Komaguchi, N. Tsunoji, M. Esmat, In Situ Blue Titania Via Band Shape Engineering for Exceptional Solar H2 Production in Rutile TiO_2, Applied Catalysis B: Environmental, Vol. 297, 2021, pp. 120380, https://doi.org/10.1016/j.apcatb.2021.120380.

[8] Z. Wang, J. Song, Y. Xu, W. Chen, M. Zhang, Treatment of MB wastewater with a Fe–RGO/TiO_2/PTFE photocatalytic Composite Membrane, New Journal of Chemistry, Vol. 12, 2024, pp. 5199-5211, https://doi.org/10.1016/j.hazadv.2024.100414.

[9] G. Guidetti, E. A. A. Pogna, L. Lombardi, F. Tomarchio, I. Polishchuk, Photocatalytic Activity of Exfoliated Graphite–TiO_2 Nanoparticle Composites, Nanoscale, Vol. 11, 2019, pp. 19301-19314, https://doi.org/10.1039/C9NR06760D.

[10] R. Wang, K. Hashimoto, A. Fujishima, M. Chikuni, E. Kojima, Light-Induced Amphiphilic

Surfaces, Nature, Vol. 388, 1997, pp. 431-432, https://doi.org/10.1038/41233.

[11] S. Takagi, S. Makuta, A. Veamatahau, Y. Otsuka, Y. Tachibana, Organic/Inorganic Hybrid Electrochromic Devices Based on Photoelectrochemically Formed Polypyrrole/TiO_2 Nanohybrid Films, Journal of Materials Chemistry, Vol. 22, 2012, pp. 22181-22189, https://doi.org/10.1039/C2JM33135G.

[12] J. Tang, J. R. Durrant, D. R. Klug, Mechanism of Photocatalytic Water Splitting in TiO_2. Reaction of Water with Photoholes, Importance of Charge Carrier Dynamics, and Evidence for Four-Hole Chemistry, Journal of the American Chemical Society, Vol. 130, 2008, pp. 13885-13891, https://doi.org/10.1021/ja8034637.

[13] O. Mekasuwandumrong, N. Jantarasorn, J. Panpranot, M. Ratova, P. Kelly, P. Praserthdam, Synthesis of Cu/TiO_2 Catalysts by Reactive Magnetron Sputtering Deposition and Its Application for Photocatalytic Reduction of CO_2 and H_2O to CH_4, Ceramics International, Vol. 45, 2019, pp. 22961-22971, https://doi.org/10.1016/j.ceramint.2019.07.340.

[14] Z. Guo, L. Zhang, H. Jiu, D. Liang, C. Wang, TiO_2-Modified Two-Dimensional Composite of Nitrogen-Doped Molybdenum Trioxide Nanosheets as a High-performance Anode for Lithium-ion Batteries, Dalton Transactions, Vol. 53, 2024, pp. 5427-5434, https://doi.org/10.1039/D3DT04176J.

[15] F. Dong, S. Guo, H. Wang, X. Li, Z. Wu. Enhancement of the Visible Light Photocatalytic Activity of C-Doped TiO_2 Nanomaterials Prepared by a Green Synthetic Approach, the Journal of Physical Chemistry C, Vol. 115, 2011, pp. 13285-13292, https://doi.org/10.1021/jp111916q.

[16] K. Arifin, R. M. Yunus, L. J. Minggu, M. B. Kassim, Improvement of TiO_2 Anotubes for Photoelectrochemical Water Splitting: Review. International Journal of Hydrogen Energy, Vol. 46, 2021, pp. 4998-5024, https://doi.org/10.1016/j.ijhydene.2020.11.063.

[17] G. Liu, P. Niu, L. Yin, H. M. Chen, α-Sulfur Crystals as a Visible-Light-Active Photocatalyst, Journal of the American Chemical Society, Vol. 134, 2012, pp. 9070-9073, https://doi.org/10.1021/ja302897b.

[18] G. Liu, P. Niu, H. M. Cheng, Visible-Light-Active Elemental Photocatalysts, Chem Phys Chem, Vol. 14, 2013, pp. 885-892, https://doi.org/10.1002/cphc.201201075.

[19] S. A. Ansari, M. H. Cho, Highly Visible Light Responsive, Narrow Band Gap TiO_2 Nanoparticles Modified by Elemental Red Phosphorus for Photocatalysis and Photoelectrochemical Applications, Scientific Reports, Vol. 6, 2016, pp. 25405, https://doi.org/10.1038/srep25405.

[20] N. O. Gopal, M. H. Basha, TiO_2 Nano-Flakes with High Aactivity Obtained from Phosphorus Doped TiO_2 Nanoparticles by Hydrothermal Method, Ceramics International, Vol. 44, 2018, pp. 22129-22134, https://doi.org/10.1016/j.ceramint.2018.08.325.

[21] R. Li, J. Batur, H. Bian, Y. J. Wang, Z. Duan, Green and Facile Fabrication of Metal Oxide/Red Phosphorus Composite Catalysts for CO_2 Photoreduction, ACS Sustainable Chemistry & Engineering, Vol. 10, 2022, pp. 8658-8668, https://doi.org/10.1021/acssuschemeng.2c02723.

[22] A. Zhou, Y. Dou, C. Zhao, J. Zhou, X. Q. Wu, J. R. Li, A Leaf-branch TiO_2/carbon@MOF Composite for Selective CO_2 Photoreduction, Applied Catalysis B: Environmental, Vol. 264, 2020, pp. 118519, https://doi.org/10.1016/j.apcatb.2019.118519.

[23] Q. Guo, L. Fu, T. Yan, W. Tian, D. Ma, Improved Photocatalytic Activity of Porous ZnO Nanosheets by Thermal Deposition Graphene-Like g-C_3N_4 for CO_2 Reduction with H_2O Vapor, Applied Surface Science, Vol. 509, 2019, pp. 144773, https://doi.org/10.1016/j.apsusc.2019.144773.

[24] X. Huang, W. Gu, S. Hu, Y. Hu, L. Zhou, Phosphorus-doped Inverse Opal g-C_3N_4 for Efficient and Selective CO Generation from Photocatalytic Reduction of CO_2, Catalysis Science & Technology, Vol. 10, 2020, pp. 3694-3670, https://doi.org/10.1039/D0CY00457J.